

# Guided bone regeneration with asymmetric collagen-chitosan membranes containing aspirin-loaded chitosan nanoparticles

Jiayu Zhang<sup>1</sup>  
 Shiqing Ma<sup>1</sup>  
 Zihao Liu<sup>1</sup>  
 Hongjuan Geng<sup>1</sup>  
 Xin Lu<sup>1</sup>  
 Xi Zhang<sup>1</sup>  
 Hongjie Li<sup>1</sup>  
 Chenyuan Gao<sup>2</sup>  
 Xu Zhang<sup>1</sup>  
 Ping Gao<sup>1</sup>

<sup>1</sup>School of Dentistry, Hospital of Stomatology, Tianjin Medical University, Tianjin, <sup>2</sup>Beijing Laboratory of Biomedical Materials, Beijing University of Chemical Technology, Beijing, People's Republic of China

**Introduction:** Membranes allowing the sustained release of drugs that can achieve cell adhesion are very promising for guided bone regeneration. Previous studies have suggested that aspirin has the potential to promote bone regeneration. The purpose of this study was to prepare a local drug delivery system with aspirin-loaded chitosan nanoparticles (ACS) contained in an asymmetric collagen-chitosan membrane (CCM).

**Methods:** In this study, the ACS were fabricated using different concentrations of aspirin (5 mg, 25 mg, 50 mg, and 75 mg). The drug release behavior of ACS was studied. Transmission electron microscopy (TEM) and scanning electron microscopy (SEM) were used to examine the micromorphology of ACS and aspirin-loaded chitosan nanoparticles contained in chitosan-collagen membranes (ACS-CCM). In vitro bone mesenchymal stem cells (BMSCs) were cultured and critical-sized cranial defects on Sprague-Dawley rats were made to evaluate the effect of the ACS-CCM on bone regeneration.

**Results:** Drug release behavior results of ACS showed that the nanoparticles fabricated in this study could successfully sustain the release of the drug. TEM showed the morphology of the nanoparticles. SEM images indicated that the asymmetric membrane comprised a loose collagen layer and a dense chitosan layer. In vitro studies showed that ACS-CCM could promote the proliferation of BMSCs, and that the degree of differentiated BMSCs seeded on CCMs containing 50 mg of ACS was higher than that of other membranes. Micro-computed tomography showed that 50 mg of ACS-CCM resulted in enhanced bone regeneration compared with the control group.

**Conclusion:** This study shows that the ACS-CCM would allow the sustained release of aspirin and have further osteogenic potential. This membrane is a promising therapeutic approach to guiding bone regeneration.

**Keywords:** aspirin, nanoparticle, drug release, membrane, guided bone regeneration

## Introduction

The inflammation of soft tissue along with progressive and irreversible bone resorption, which can cause tooth loss and the failure of implants around bone defect, may be caused by periodontitis and peri-implantitis.<sup>1-3</sup> Currently, guided bone regeneration (GBR) is frequently used to repair bone defects and this method has achieved considerable success.<sup>4</sup> GBR membranes are used as barriers to isolate the periodontal bone defects from gingival connective tissue so that the newly formed bone can grow along the edge of the alveolar bone defect.<sup>5</sup> It should be noted that current GBR membranes just act as barriers and do not actively accelerate bone reconstruction. GBR membranes, which are capable of promoting faster bone regeneration and releasing relevant therapeutic drugs, are proposed to be highly effective for periodontal regeneration.<sup>6</sup> More

Correspondence: Xu Zhang; Ping Gao  
 School of Dentistry, Hospital of Stomatology, Tianjin Medical University,  
 12 Observatory Road, Tianjin 300070,  
 People's Republic of China  
 Email zhangxu@tmu.edu.cn;  
 gaoping@tmu.edu.cn

recent studies have focused on developing GBR membranes with asymmetric structures instead of developing an asymmetric GBR membrane with drugs loaded throughout the membrane.<sup>7,8</sup> Accordingly, a membrane that can stimulate faster bone growth would be very promising.<sup>9</sup>

Chitosan (poly-1,4-D-glucosamine), a deacetylated derivative of chitin, is a rare alkaline polysaccharide with a positive charge found in nature. It is well-known for its excellent biodegradability and biocompatibility, as well as its low toxicity.<sup>10</sup> Additionally, because it can easily be processed into nanofibers, gels, scaffolds, membranes, and nanoparticles, chitosan has received widespread attention recently.<sup>11</sup> Collagen type I is the most significant and abundant structural protein in connective tissues and is a promising scaffold material for tissue engineering.<sup>12,13</sup> Although collagen may undergo a high rate of rapid degradation after contact with body fluids, cross-linking can be used to improve the physical properties of collagen.<sup>14</sup> In this study, asymmetric membranes were fabricated with cross-linked collagen type I, chitosan, and chitosan nanoparticles, and the membranes played pivotal roles in the cell adhesion, proliferation, and differentiation.

Generally, drugs are blended directly into the matrix of GBR membranes, which causes rapid release of the drugs from the membranes, resulting in a high burst release and short release period;<sup>6</sup> however, nanotechnology can solve this problem. Thus, there is a strong push to develop sustained and controlled drug delivery systems (DDS) for GBR applications.<sup>6</sup> Targeted and controllable release are the most important characteristics of nanoparticle-based DDS. Controllable release means that the loaded drugs can be liberated in the right place and at the right time, which would mean a concomitant reduction in administration times and avoid toxicity to other organs.<sup>15</sup> DDS, such as polymer- and lipid-based nanoparticles, can be designed to improve the pharmacological and therapeutic properties of drugs administered parentally.<sup>16</sup> To avoid drug-associated complications, natural polymers have become the optimal materials for the preparation of nanoparticles due to their biodegradable nature.<sup>17</sup> Chitosan has been widely investigated in the development of controlled-release DDS because it makes it easier for drugs to be absorbed transmucosally due to its positive charges electrostatically interacting with the negatively charged mucosal surface.<sup>18</sup> Thus, in this research, chitosan was chosen to prepare the nanoparticles through ionic gelation, which is based on the assembly of positively charged chitosan and negatively charged sodium tripolyphosphate (TPP).

Aspirin (acetylsalicylic acid) has been widely used for decades as a non-steroidal anti-inflammatory drug (NSAID),

and it plays important roles in various biological pathways, such as inhibition of the enzyme COX-2.<sup>19,20</sup> Recent research has revealed that aspirin may modulate the balance between bone resorption and bone formation in ovariectomy-induced osteoporosis, and can accelerate bone repair in rodents and inhibit the differentiation and maturity of osteoclasts.<sup>21–23</sup> When inflammatory tissue exists, bone mesenchymal stem cells (BMSCs) have exhibited impaired immunoregulatory properties.<sup>19</sup> Nevertheless, aspirin could significantly enhance the immunoregulatory properties of BMSCs by up-regulating regulatory T cells and down-regulating Th17 cells via the 15d-PGJ<sub>2</sub>/PPAR $\gamma$ /TGF- $\beta$ 1 pathway.<sup>19</sup> However, systemic drugs, repeatedly used over a long period of time, have potential side effects and may lead to the development of bacterial resistance and local inadequate drug concentrations in the periodontal tissue and gingival crevicular fluid.<sup>24</sup> The long-term use of aspirin may cause side effects in the gastrointestinal tract including hemorrhagic micro-bleeding and gastric erosion;<sup>25,26</sup> and low-dose and topical applications of aspirin to treat disease would be very promising. An aspirin-loaded chitosan nanoparticle has been prepared and used to demonstrate that aspirin can be slowly and controllably released from the composite particles *in vitro*.<sup>18</sup>

The objective of this study was to develop an asymmetric GBR membrane containing aspirin-loaded chitosan nanoparticles (ACS) for the local delivery and sustained release of aspirin. We hypothesized that these aspirin-loaded chitosan nanoparticles contained in collagen-chitosan membranes (ACS-CCM) can keep soft tissue from invading bone defects while, at the same time, promoting bone regeneration. The nanoparticles were characterized in terms of morphology and *in vitro* release; the morphology, biodegradation, and cytocompatibility of the membranes were investigated. A rat skull bone defect model was established to examine impact of the membranes on bone regeneration behavior.

## Materials and methods

### Materials

Chitosan (87% deacetylated), TPP, and glacial acetic acid were purchased from Life Science Products & Services (Shanghai, People's Republic of China). EDC (1-ethyl-3-(3-dimethylaminopropyl)-carbodiimide) and NHS (N-hydroxysuccinimide) were purchased from Sigma-Aldrich Co. (St Louis, MO, USA). Cell Counting Kit-8 (CCK-8) and Live/Dead cell double staining kits were obtained from Solarbio (Beijing, People's Republic of China). ALP assay kits were purchased from NJCBIO (Nanjing, People's Republic of China).

## Preparation of aspirin-loaded nanoparticles

In the first stage, chitosan was dissolved in 1% (v/v) aqueous acetic acid to obtain a 0.2% (w/v) chitosan solution. Various amounts of aspirin (5 mg, 25 mg, 50 mg, and 75 mg) were added to anhydrous ethanol to generate the saturated solutions, which were then individually added to samples of the 0.2% chitosan solution. Subsequently, 2% (w/v) aqueous TPP solution was added dropwise to the chitosan–aspirin solution under vigorous magnetic stirring. After stirring for 10 minutes, the final mixture was centrifuged at 1,500 rpm for 30 minutes. Finally, ACS were washed repeatedly with distilled water and then freeze-dried.

## In vitro release of aspirin

The ACS were dispersed in PBS (pH 7.4) at 37°C under magnetic stirring in a constant temperature oscillator (100 rpm). At various time points (1, 3, 5, 7, 10, and 14 days), the supernatant was collected, and 2 mL samples were taken out and replaced with the same volume of new fresh medium. The amount of released aspirin was measured with ultraviolet spectrophotometry (BioSpectrometer, Eppendorf, Germany) at 280 nm (n=3). The concentrations of aspirin were calculated by comparison to a standard curve.

## Fabrication of asymmetric CCM preparation

Collagen was isolated from Sprague-Dawley (SD) rat tail tendons dissolving in 0.5 M acetic acid at 4°C for 2 days. Then, the collagen solution was centrifuged in a refrigerated centrifuge (3,000 rpm at 4°C for 30 minutes), and the pH of the solution was adjusted to 5.0 with 0.1 M NaOH. ACS (10 mg) were added to 10 mL of the collagen solution and solution of EDC and NHS (3:1) was added as a cross-linker, and the mixture was allowed to react for 30 minutes at room temperature to afford the final collagen mixture. Then, 1 mL of the 2% (w/v) chitosan solution was poured into a polytetrafluoroethylene mold (10 mm in diameter, 1.5 mm in depth) and heated at 45°C for 1 hour. Next, the chitosan membrane was immersed into the NaOH solution and then washed repeatedly with distilled water until the membrane reached a neutral pH. Subsequently, 1.5 mL of the collagen mixture was poured onto the pure chitosan membrane, which was then frozen and lyophilized to generate asymmetric ACS-CCM.

In the meantime, pure chitosan membranes, pure collagen membranes, and cross-linked collagen membranes were prepared with the same method. The pure collagen membrane was prepared without a cross-linker.

## Morphology of aspirin-loaded nanoparticles and CCM

The morphology of ACS was examined by transmission electron microscopy ([TEM], JEM-2100F; JEOL, Tokyo, Japan). The nanoparticles were uniformly immersed in collagen solution and then dropped on copper grids (400 mesh size), dried at room temperature, and then examined using TEM. The average particle dimensions of the nanoparticles were characterized by the dynamic light scattering (DLS) technique.

The morphological characteristics of the ACS-CCM were observed using scanning electron microscopy ([SEM]; Nova NanoSEM 430, FEI, Hillsboro, OR, USA). The obverse side, the reverse side, and the cross-section were all examined. Before observation, the membranes were sputter-coated with gold under an argon atmosphere using a sputter coater (K575XD, Emitech, Quorum Technologies Ltd., East Sussex, UK).

## Biodegradation of the membranes in vitro

The pure chitosan membranes, pure collagen membranes, cross-linked collagen membranes, and the ACS-CCM were immersed in simulated body fluid and incubated at 37°C. After soaking for 7, 14, 21, and 28 days, the samples were taken out of the medium, washed with distilled water, lyophilized, and weighed. The degradation rate is expressed as the percentage of the relative weight loss of the samples based on the following equation:

$$D = \frac{W - W_t}{W} \times 100\%$$

where  $D$  represents mass lost,  $W$  is the initial weight of the membrane, and  $W_t$  is the weight after different amounts of degradation. Each experiment was repeated three times.

## Cell proliferation

The ACS-CCM were cut into disks, 15 mm in diameter, to match the well size of a 24-well plate and then sterilized using a 25 kGy dose of gamma radiation (cobalt-60) (Huanming Gaoke Fuzhao Co., Tianjin, People's Republic of China). The different membranes were pre-wetted with complete growth medium (DMEM with 10% FBS, 100 mg/mL streptomycin, and 100 U/mL penicillin). Then,  $1 \times 10^4$  BMSCs in 1,000  $\mu$ L of medium were seeded onto the membrane disks (n=3) and cultured in 24-well plates, which were maintained in a 5% CO<sub>2</sub> incubator at 37°C.

To determine the cell proliferation on different membranes, 10  $\mu\text{L}$  of CCK-8 solution and 90  $\mu\text{L}$  of fresh medium were added to each well to replace the original culture medium after aliquots were removed at various culturing intervals (1, 3, 5, and 7 days). The plates were then incubated in the 5%  $\text{CO}_2$  incubator at 37°C for 4 hours. Subsequently, samples of the supernatant solutions were transferred to a new 96-well plate, and the absorbance of each sample was measured at 450 nm using a Microplate Reader (RT-6000, Rayto, Guangdong, People's Republic of China).

### Live/Dead cell double staining

To observe the morphology of cells seeded on each membrane, Live/Dead cell double staining was carried out. The membranes were removed from the 24-well plates after 3 and 5 days, washed with PBS three times, placed in new plates, and then stained with an acridine orange/ethidium bromide solution (100  $\mu\text{L}$  per well). The cells on the sample membranes were observed by laser confocal microscopy (LSCM) (Fv-1000, Olympus Corporation, Tokyo, Japan).

### ALP activity

To study the differentiation of BMSCs at various time points, ALP experiments were performed. BMSCs seeded onto different membranes ( $n=3$ ) were cultured in growth medium (DMEM supplemented with 10% FBS, 10 mmol/L sodium  $\beta$ -glycerophosphate, 50 mg/L vitamin C, and  $10^{-8}$  mol/L dexamethasone). On the 7th and 14th day after cell lysis, ALP activity was determined using an ALP assay kit.

### Animal study

An animal study was performed to evaluate the bone regeneration behavior of different membranes *in vivo*; to do this, a skull defect model of SD rats was established. The investigation conformed to the regulations of the experimental animal administration issued by the Ministry of Science and Technology of China (<http://www.most.gov.cn>), and the protocol was evaluated and accepted by the Institutional Ethics Committee of the Tianjin Medical University before the animal experiments. The 8-week-old rats (260–320 g, male) were divided into a control group and a 50 mg ACS-CCM group. The rats were anesthetized by an intraperitoneal injection of chloral hydrate (1 mg/330 g; Yulong, Yangshuo, People's Republic of China). After exposure of the parietal calvarium, a full-thickness skull defect (5 mm in diameter) was generated with a trephine bur driven by a hand-piece, which was cooled by continuously dripping sterile saline. Subsequently, the different membranes (5 mm in diameter) were implanted

into the defects. In the control group, the defects were covered without the membranes. The periosteum and skin were closed with sutures using a 5-0 suture line.

### Micro-computed tomography (micro-CT) scanning evaluation

Micro-CT scans were performed to investigate bone regeneration *in situ* using a micro-CT scanner (Sky Scan 1174v2, SkyScan N.V., Kontich, Belgium). After 1 and 2 months, the animals were euthanized by injecting an overdose of pentobarbital sodium. Then, the bone defects with surrounding cranial tissues were removed from the bodies. The samples were fixed in 10% neutral-buffered formalin and then scanned over 360° of rotation under an X-ray voltage of 50 KV.

### Histological preparation and evaluation

The samples were decalcified in a hydrochloric acid-formaldehyde solution, then dehydrated in an ascending graded series of alcohol, and embedded in paraffin. In the center of the bone defects, a series of 5  $\mu\text{m}$  transverse sections were prepared and stained with hematoxylin and eosin (H&E) for observation by light microscopy (BX51, Olympus Corporation).

### Statistical analysis

All quantitative data were expressed as the mean  $\pm$  standard deviation. Statistical analysis of the results was performed using Student's *t*-test.  $P<0.05$  was considered to indicate statistical significance.

## Results

### Drug release of aspirin-loaded nanoparticles *in vitro*

The release of aspirin *in vitro* is presented in Figure 1. The calibration curves of the absorbance of aspirin at 298 nm showed an  $R^2=0.998$ . A burst release of aspirin was observed on the first day followed by a gradual release until day 14, which indicated that the ACS performed well in controlling the release of the drug.

### Characterization of chitosan/collagen membrane

Figure 2 shows the TEM images and the DLS result of the ACS. The nanoparticles were spherical with smooth surfaces and were approximately 90 nm in size. As shown in Figure 3, the cross-section of the ACS-CCM showed an asymmetric structure (Figure 3C), including a dense layer and a loose



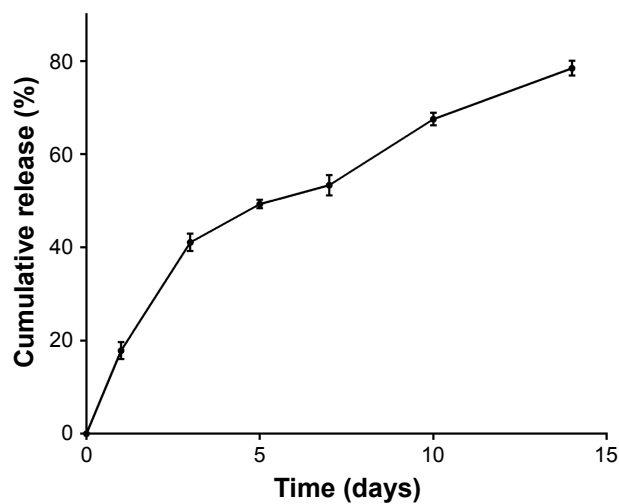


**Figure 1** Release curve of ACS at 1, 3, 5, 7, 10, and 14 days.  
**Note:** There is a burst release on the first day, and then a sustained release is observed until day 14, (n=3).  
**Abbreviation:** ACS, aspirin-loaded chitosan nanoparticles.

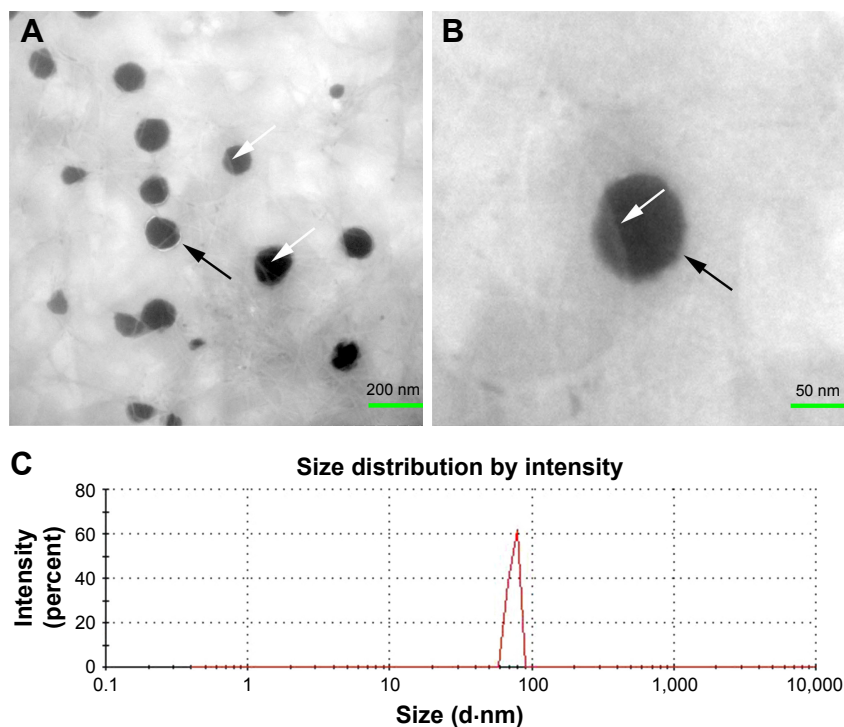
layer. The surface of the collagen layer and the chitosan layer is shown in Figure 3A and B. Figure 3D shows a schematic diagram of the cross-section of the membrane. The loose layer of the asymmetrical membrane can improve cell adhesion while the dense layer can effectively isolate the bone defect from the invasion of surrounding connective fibrous tissues.

The degradation rates of the membranes in vitro are shown in Figure 4. The ACS-CCM had a lower degradation rate than pure collagen membranes and cross-linked collagen membranes, but it was higher than that of pure chitosan membranes. Even after 28 days of soaking, ACS-CCM maintained a low rate of degradation. All membranes showed weight loss with increased immersion time.

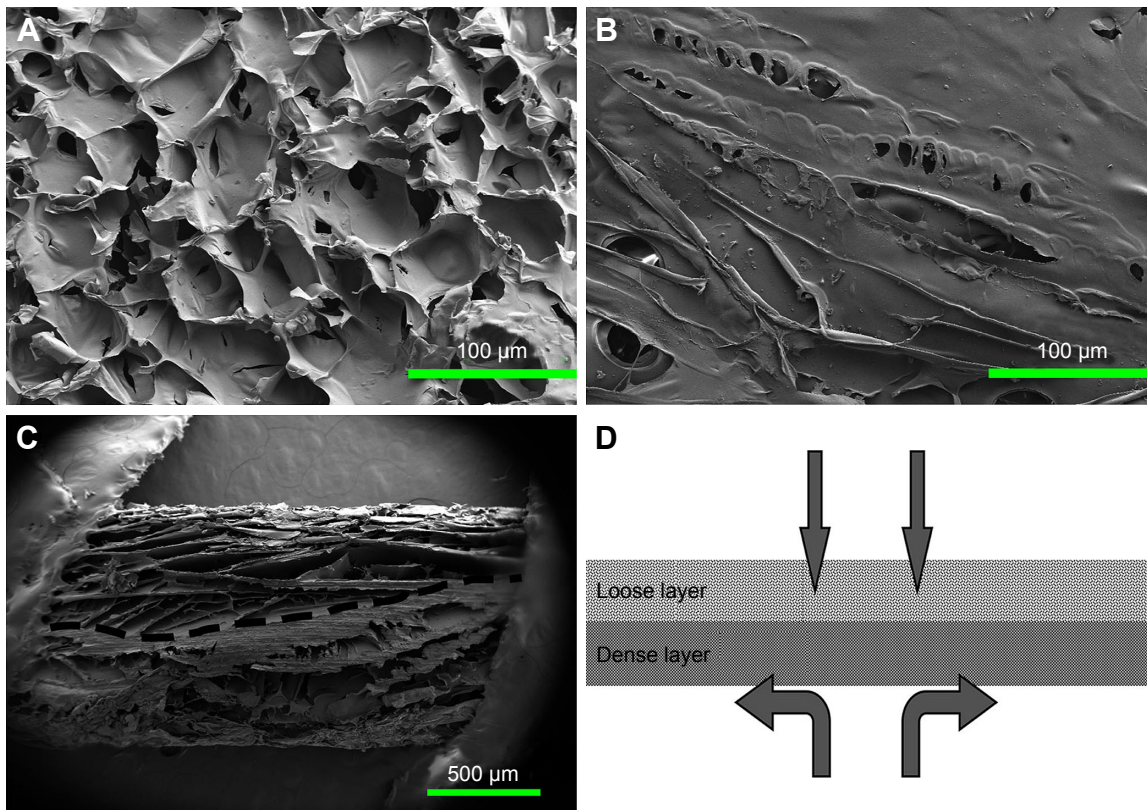
### Evaluation of biocompatibility in vitro

Figure 5 presents the results of the CCK-8 assay of the BMSC cells seeded on the five different kinds of membranes after 1, 3, 5, and 7 days. Compared with the other membranes, the absorbance of the 50 mg ACS-CCM group exhibited a statistically significant difference at a certain time interval ( $P < 0.05$ ), which indicates that the 50 mg ACS-CCM group had more beneficial properties to assist in the growth of BMSCs.

The ALP activities of BMSCs distributed on different membranes on the 7th and 14th day after seeding are shown in Figure 6. The 25 mg and 50 mg ACS-CCM groups both showed a significant increase in ALP activity compared with that of the other membranes. The 50 mg ACS-CCM group exhibited a higher ALP activity on the 7th day and the highest activity with even longer culture times, which indicated obvious growth.



**Figure 2** TEM and DLS characterization of ACS.  
**Notes:** (A, B) The TEM image shows ACS dispersed in collagen solution, the black arrow indicates the ACS, and the white arrows show the collagen fibrils. (C) DLS result shows the ACS size distribution.  
**Abbreviations:** TEM, transmission electron microscopy; DLS, dynamic light scattering; ACS, aspirin-loaded chitosan nanoparticles.



**Figure 3** SEM images showing the morphologies of the ACS-CCM.

**Notes:** (A) Image of the loose cross-linked collagen layer, (B) the dense chitosan layer, (C) the cross-section of the ACS-CCM, and (D) a schematic diagram of the cross-section.

**Abbreviations:** SEM, scanning electron microscopy; ACS-CCM, aspirin-loaded chitosan nanoparticles contained in collagen-chitosan membranes.

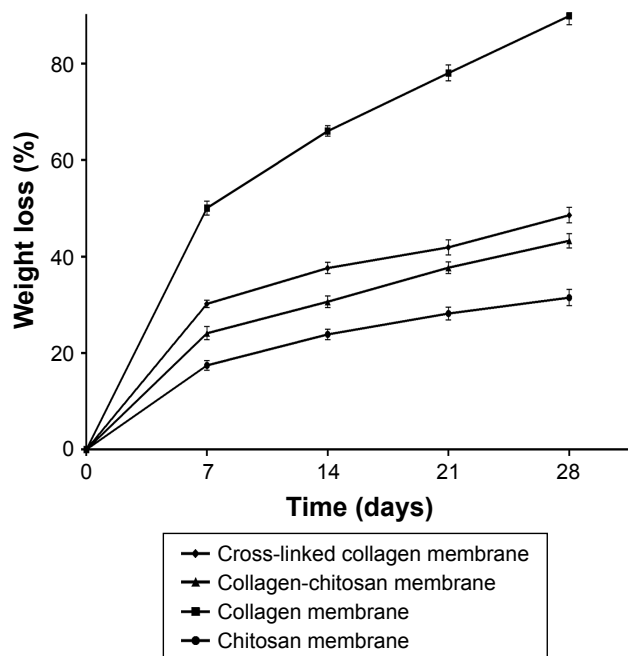


**Figure 4** Weight loss of membranes during different soaking intervals.

**Notes:** The image shows the difference in the degradation rates among the four groups. The cross-linked collagen membranes degraded slower than the collagen membranes (n=3).

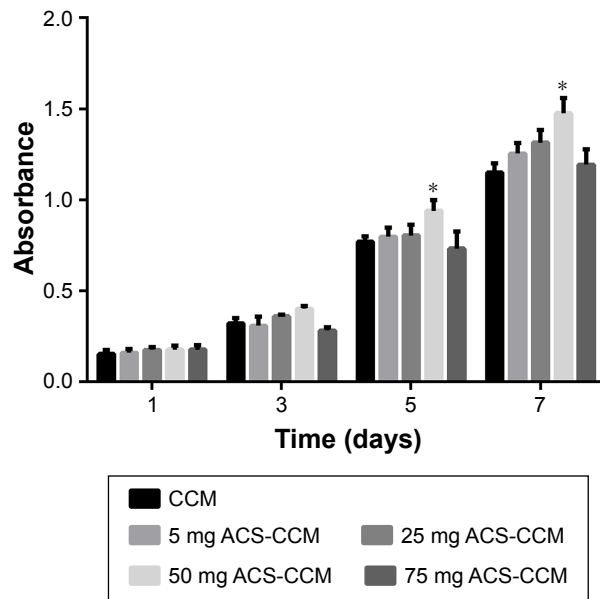


**Figure 5** CCK-8 assay results of BMSCs distributed on different membranes after culturing for 1, 3, 5, and 7 days.

**Note:** There was a statistically significant difference in cell proliferation between the 50 mg ACS-CCM group and the other four groups on day 5 (\* $P < 0.05$ , n=3).

**Abbreviations:** CCK-8, Cell Counting Kit-8; BMSCs, bone mesenchymal stem cells; CCM, collagen-chitosan membranes; ACS-CCM, aspirin-loaded chitosan nanoparticles contained in collagen-chitosan membranes.

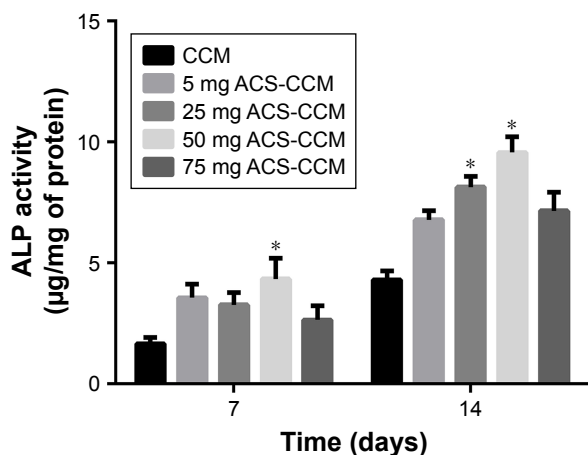


**Figure 6** ALP activities of BMSCs growing in different membranes after culturing for 7 and 14 days.

**Note:** The difference between the ALP activity of the 50 mg ACS-CCM group and the other groups was statistically significant at each testing time point (\* $P < 0.05$ ,  $n = 3$ ).

**Abbreviations:** BMSCs, bone mesenchymal stem cells; CCM, collagen-chitosan membranes; ACS-CCM, aspirin-loaded chitosan nanoparticles contained in collagen-chitosan membranes.

## Live/Dead assay

The osteoblasts on the surface of the CCM were stained by the Live/Dead cell double staining kit and characterized using LSCM (Figure 7). The representative LSCM images showed that after culturing for 3 and 5 days, the osteoblasts

on the 50 mg ACS-CCM sample presented favorable cell morphology. This result indicated that the 50 mg ACS-CCM samples showed the same cell morphology as the CCM without the nanoparticles, and both membranes could maintain satisfactory cell viability.

## Result of osteogenic potential in vivo

The diameter of the penetrating calvarial defects of the rats was 5 mm (Figure 8). The result of 3D reconstruction and micro-CT of the specimens (Figure 9) at 4 and 8 weeks showed markedly more new bone formation in 50 mg ACS-CCM group than that of the control group at the macro level. This result indicates that the 50 mg ACS-CCM samples have a higher bone regeneration rate than the control group. Figure 10 shows the H&E staining of the histological sections. Eight weeks after implantation, the structure of the ACS-CCM could not be observed; the membrane was almost degraded and integrated into adjacent fibrous tissue.

## Discussion

The current therapies for periodontitis and peri-implantitis focus on antimicrobial treatment and the regeneration of lost bone tissue.<sup>27,28</sup> However, bone regeneration remains a more

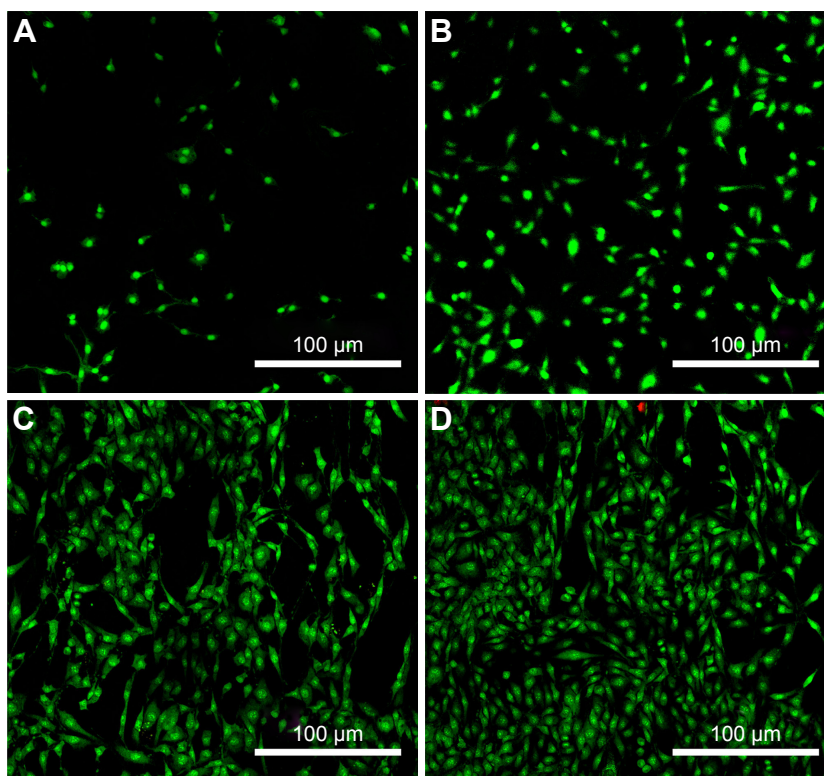


**Figure 7** LSCM images of BMSCs attached to the collagen surface after culturing for 3 and 5 days (AO/EB staining).

**Note:** The LSCM images showed no differences in cell morphology between the CCM group (3 days [A] and 5 days [C]) and the 50 mg ACS-CCM group (3 days [B] and 5 days [D]).

**Abbreviations:** BMSCs, bone mesenchymal stem cells; LSCM, laser scanning confocal microscopy; AO/EB, acridine orange/ethidium bromide; ACS-CCM, aspirin-loaded chitosan nanoparticles contained in collagen-chitosan membranes; CCM, collagen-chitosan membranes.



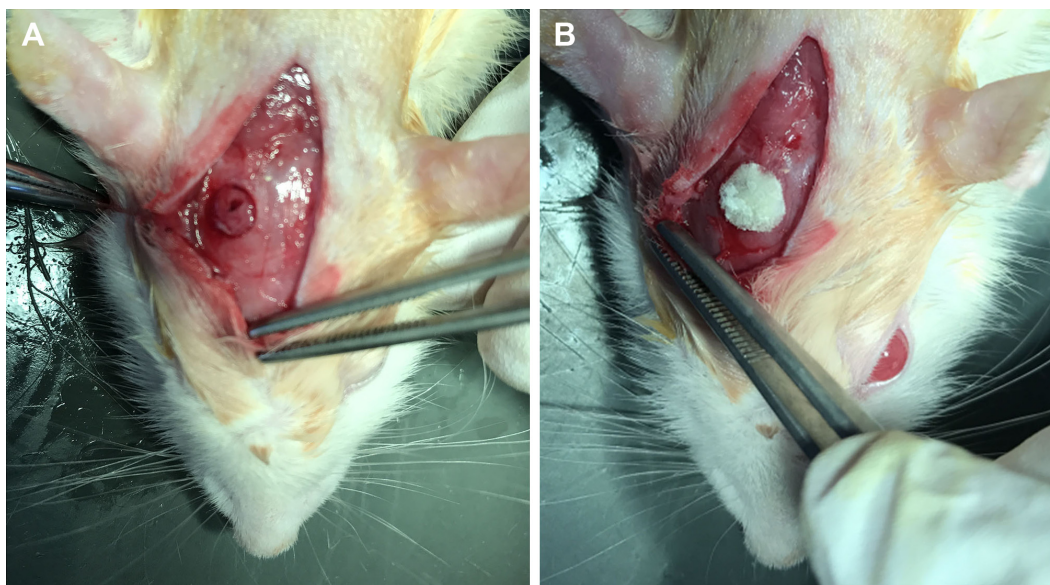


**Figure 8** Skull-penetrating defect model of SD rats.

**Notes:** (A) The parietal calvarium defect of SD rat. (B) 50 mg ACS-CCM implanted in the defect.

**Abbreviations:** SD, Sprague-Dawley; ACS-CCM, aspirin-loaded chitosan nanoparticles contained in collagen-chitosan membranes.

challenging issue in the field of periodontal therapies. Many studies have indicated that some NSAIDs are commonly used in the repair of bone tissue, especially in bone healing and the treatment of bone fractures.<sup>29–31</sup> Moreover, NSAIDs have also been shown to reduce the severity of tissue destruction and bone loss caused by periodontal disease.<sup>27,32</sup> Nevertheless, NSAIDs may have an adverse effect on osteoblast proliferation, and the dose of the NSAIDs is the critical factor in the cell proliferation, differentiation, and migration.<sup>30,33</sup>

Compared with the systemic approach, local DDS are more favorable for a number of reasons, including its various advantages, such as site-specific delivery, decreased dosage frequency, reduction in gastrointestinal side effects, and minimized chance of bacterial resistance.<sup>34</sup> Chitosan

nanoparticles are becoming a promising drug delivery device.<sup>35</sup> In this study, ACS were successfully prepared by an emulsion-cross-linking method, and TPP was used as the cross-linker. The mechanisms by which drugs are released from polymer encapsulation include diffusion and polymer degradation.<sup>36</sup> When aspirin was released from the chitosan nanoparticles, the initial release concentration was higher, which was due to diffusion of the drug from the surface of the nanoparticles. In addition, late in the release process, the concentration of aspirin was lower but aspirin continued to be released until the 14th day (Figure 1), at which point its release may be from both diffusion and polymer degradation. This result indicated that the nanoparticles fabricated in this research could achieve controlled drug release.

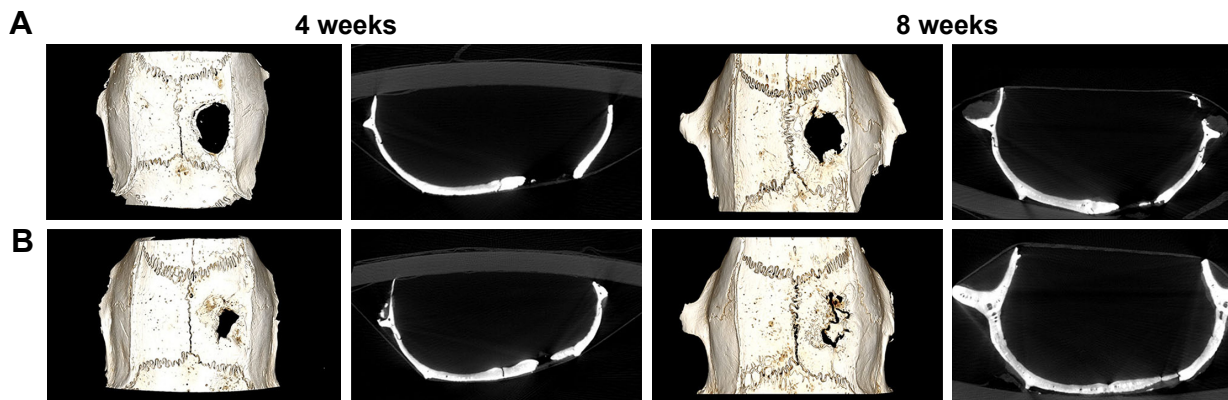


**Figure 9** 3D reconstruction and micro-CT images of new bone regeneration after 4 and 8 weeks.

**Note:** The 3D reconstructions and the coronal sections of rat craniums in (A) the control and (B) the 50 mg ACS-CCM group after being implanted for 4 and 8 weeks.

**Abbreviations:** micro-CT, micro-computed tomography; ACS-CCM, aspirin-loaded chitosan nanoparticles contained in collagen-chitosan membranes.



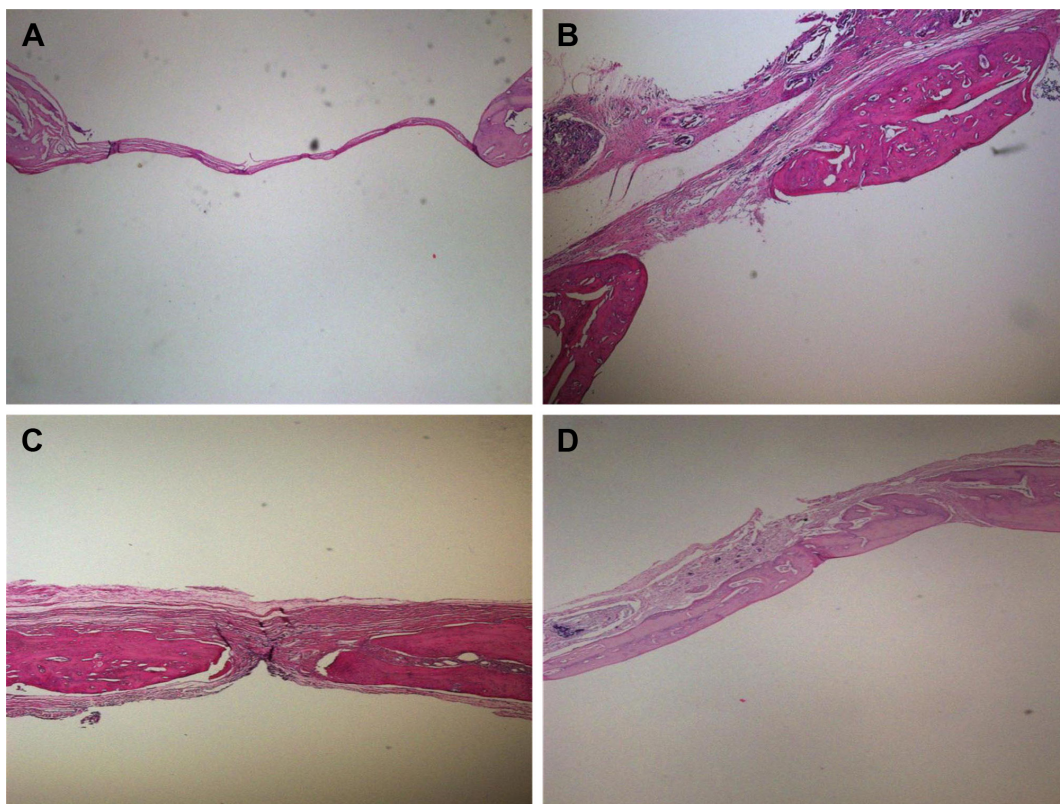


**Figure 10** H&E staining of SD rat cranial defects at different time points.

**Notes:** (A) Control group and (B) 50 mg ACS-CCM at 4 weeks. (C) Control group and (D) 50 mg ACS-CCM group at 8 weeks.

**Abbreviations:** H&E, hematoxylin and eosin; SD, Sprague-Dawley; ACS-CCM, aspirin-loaded chitosan nanoparticles contained in collagen-chitosan membranes.

The scaffolds must degrade after implantation because it promotes the formation of new bone.<sup>37</sup> Collagen is widely used as a biomaterial due to its perfect biocompatibility, biodegradability, and biological activities.<sup>38,39</sup> However, the rapid degradation and poor mechanical properties of collagen limit its use. The degradation rate and the mechanical properties may influence the long-term success of bone tissue regeneration due to the untimely stress it places on the new bone, which is detrimental for the regeneration of tissue.<sup>40</sup> Membranes need to be porous, which allows cells to distribute widely and allows more efficient mass transport for oxygen, nutrients, growth factors, and waste products, but in the meantime, suitable rigidity is required to resist the surrounding mechanical stresses during the tissue regeneration period.<sup>41</sup> However, the collagen lacks mechanical strength and easy to be degraded,<sup>42</sup> which may be due to its porosity. Cross-linking methods can enhance the mechanical properties of collagen by incorporating another material,<sup>43</sup> and reducing the degradation rate of collagen to match the speed of tissue regeneration. As shown in Figure 4, the cross-linked collagen membranes showed lower degradation rates than the pure collagen membranes. Thus, an asymmetric membrane was fabricated with cross-linked collagen containing ACS

for the loose layer and chitosan, which is slow to degrade, for the dense layer (Figure 3).

A major concern of drugs released from GBR membranes is that the drug should not interfere with cellular activities. In the present study, the cell proliferation and osteogenic activity of different membranes in vitro was examined with BMSCs. A previous study showed that aspirin at high concentrations may have an anti-proliferative effect on BMSCs, but a low concentration (200  $\mu\text{g/mL}$ ) did not induce the apoptosis of BMSCs.<sup>19</sup> Moreover, a low dose of aspirin can promote BMSCs' proliferation.<sup>44</sup> The ACS-CCM prepared in this study showed satisfactory cytocompatibility and could promote the adhesion and proliferation of BMSCs (Figure 5). In addition, the number of cells on the 50 mg ACS-CCM samples was considerably higher than that on the other membranes.

Previous research suggested that aspirin therapy can enhance the telomerase activity in stem cells and increase the telomere length of BMSCs, which may improve stem cells' functioning, promote their survival, and cause the therapeutic effects of stem cells.<sup>21</sup> In the meantime, aspirin augmented the expression of ALP and facilitated the degradation of phospho- $\beta$ -catenin, leading to increased activity in the Wnt signaling pathway, which is a recognized pathway

in osteogenesis.<sup>21,45</sup> ALP is a recognized biochemical marker for osteogenesis activity, therefore the ALP levels were examined at different time points (7 and 14 days) to observe the changes. The ALP activity on the 50 mg ACS-CCM samples was higher than that of the other membranes on the 7th day. With the release of aspirin, the 50 mg ACS-CCM group showed a higher ALP activity among the different kinds of membranes until the 14th day, indicating a better bone formation ability (Figure 6).

The animal experiment was used to evaluate the bone regeneration behavior of the asymmetric ACS-CCM. Defects of 5 mm in diameter were selected based on the critical size of defects defined by Schmitz and Hollinger.<sup>46</sup> Previous studies suggested that within BMSCs-mediated bone formation, the inhibitory function of IFN- $\gamma$  might be a result of a synergistic effect with TNF- $\alpha$ , which activates a Fas-signaling-mediated death pathway to enhance BMSCs' apoptosis.<sup>47</sup> However, aspirin could significantly promote BMSCs-based bone regeneration by inhibiting the levels of TNF- $\alpha$  and IFN- $\gamma$ , and reverse the proinflammatory cytokine-induced osteogenic deficiency of BMSCs.<sup>47</sup> After being implanted for 4 and 8 weeks, the 3D reconstruction and micro-CT results illustrated that the control group showed lower new bone regeneration than the 50 mg ACS-CCM group (Figure 9). To observe the histological differences between the 50 mg ACS-CCM group and the control group, H&E staining was performed (Figure 10), which confirmed the micro-CT results. Histological analysis showed no signs of foreign-body reactions or acute inflammation, and preferable bone formation was observed in the 50 mg ACS-CCM group. Both the micro-CT result and the histological analysis all indicated that the 50 mg ACS-CCM had good biological compatibility and osteoconductive effects.

The long-term and repeated use of systemic drugs has potential side effects and may bring about the development of bacterial resistance and inadequate antibiotic concentrations.<sup>24</sup> Therefore, DDS are becoming an increasingly popular way to overcome these disadvantages. The development of a wide range of nanotechnologies is beginning to change the traditional therapeutic methods. At present, most studies of nanoparticles have been focused on tumor therapy, and only few experiments have focused on osteogenic regeneration. Previous studies indicated that further improvements in GBR techniques can be achieved using bioactive membranes which can accelerate bone formation.<sup>48</sup> Therefore, ACS-CCM were fabricated in this study to control the release of drugs and promote bone regeneration. The results in this study suggest that ACS-CCM have the potential to be used as GBR membranes in clinical applications, although the practical use of

ACS-CCM will be determined by further studies. However, BMSCs from different species or tissues may show different dose responses when treated with aspirin.<sup>19</sup> The optimal concentration of aspirin to promote human BMSCs also remains to be determined.

## Conclusion

In this study, asymmetric ACS-CCM were developed. The results indicated that the ACS achieved a desirable controlled-release pattern, and the fabricated membranes showed good biocompatibility and osteogenic potential. The membranes also significantly increased new bone formation in a rat calvarial defect model. Therefore, the asymmetric ACS-CCM fabricated in this study may fulfill clinical requirements.

## Acknowledgments

This study was supported by grants from National Natural Science Foundation of China (no 31470919, no 81701019 and no 81501798) and the Scientific Research Fund of Tianjin Medical University (no 2016KYZQ16). We thank Xiao Chen of the Stomatological Hospital of The Fourth Military Medical University for his contributions.

## Disclosure

The authors report no conflicts of interest in this work.

## References

1. Liu Y, Zheng Y, Ding G, et al. Periodontal ligament stem cell-mediated treatment for periodontitis in miniature swine. *Stem Cells*. 2008;26(4):1065–1073.
2. Chen FM, Zhang J, Zhang M, An Y, Chen F, Wu ZF. A review on endogenous regenerative technology in periodontal regenerative medicine. *Biomaterials*. 2010;31(31):7892–7927.
3. Pihlstrom BL, Michalowicz BS, Johnson NW. Periodontal diseases. *Lancet*. 2005;366(9499):1809–1820.
4. Bashutski JD, Wang HL. Periodontal and endodontic regeneration. *J Endod*. 2009;35(3):321–328.
5. Zhang K, Zhao M, Cai L, Wang Zk, Sun Yf, Hu QL. Preparation of chitosan/hydroxyapatite guided membrane used for periodontal tissue regeneration. *Chinese Journal of Polymer Science*. 2010;28(4):555–561.
6. Li W, Ding Y, Yu S, Yao Q, Boccaccini AR. Multifunctional chitosan-45S5 bioactive glass-poly(3-hydroxybutyrate-co-3-hydroxyvalerate) microsphere composite membranes for guided tissue/bone regeneration. *ACS Appl Mater Interfaces*. 2015;7(37):20845–20854.
7. Cho WJ, Kim JH, Oh SH, Nam HH, Kim JM, Lee JH. Hydrophilized polycaprolactone nanofiber mesh-embedded poly(glycolic-co-lactic acid) membrane for effective guided bone regeneration. *J Biomed Mater Res A*. 2009;91(2):400–407.
8. Oh SH, Kim JH, Kim JM, Lee JH. Asymmetrically porous PLGA/Pluronic F127 membrane for effective guided bone regeneration. *J Biomater Sci Polym Ed*. 2006;17(12):1375–1387.
9. Xu C, Lei C, Meng L, Wang C, Song Y. Chitosan as a barrier membrane material in periodontal tissue regeneration. *J Biomed Mater Res B Appl Biomater*. 2012;100(5):1435–1443.
10. Shan L, Tao EX, Meng QH, et al. Formulation, optimization, and pharmacodynamic evaluation of chitosan/phospholipid/beta-cyclodextrin microspheres. *Drug Des Devel Ther*. 2016;10:417–429.

11. Jayakumar R, Prabakaran M, Nair SV, Tamura H. Novel chitin and chitosan nanofibers in biomedical applications. *Biotechnol Adv*. 2010; 28(1):142–150.
12. Islam A, Younesi M, Mbimba T, Akkus O. Collagen substrate stiffness anisotropy affects cellular elongation, nuclear shape, and stem cell fate toward anisotropic tissue lineage. *Adv Healthc Mater*. 2016;5(17): 2237–2247.
13. Ma L, Gao C, Mao Z, Zhou J, Shen J, Hu X, Han C. Collagen/chitosan porous scaffolds with improved biostability for skin tissue engineering. *Biomaterials*. 2003;24(26):4833–4841.
14. Ma S, Adayi A, Liu Z, et al. Asymmetric collagen/chitosan membrane containing minocycline-loaded chitosan nanoparticles for guided bone regeneration. *Sci Rep*. 2016;6:31822.
15. Wang YF, Liu L, Xue X, Liang XJ. Nanoparticle-based drug delivery systems: What can they really do in vivo? *F1000Res*. 2017;6:681.
16. Allen TM, Cullis PR. Drug delivery systems: entering the mainstream. *Science*. 2004;303(5665):1818–1822.
17. Kumari A, Yadav SK, Yadav SC. Biodegradable polymeric nanoparticles based drug delivery systems. *Colloids Surf B Biointerfaces*. 2010; 75(1):1–18.
18. Shi Y, Wan A, Shi Y, Zhang Y, Chen Y. Experimental and mathematical studies on the drug release properties of aspirin loaded chitosan nanoparticles. *Biomed Res Int*. 2014;6:133–140.
19. Tang J, Xiong J, Wu T, et al. Aspirin treatment improved mesenchymal stem cell immunomodulatory properties via the 15d-PGJ2/PPARgamma/TGF-beta1 pathway. *Stem Cells Dev*. 2014;23(17):2093–2103.
20. Tosco P, Lazzarato L. Mechanistic insights into cyclooxygenase irreversible inactivation by aspirin. *ChemMedChem*. 2009;4(6):939–945.
21. Yamaza T, Miura Y, Bi Y, et al. Pharmacologic stem cell based intervention as a new approach to osteoporosis treatment in rodents. *PLoS One*. 2008;3(7):e2615.
22. Le Blanc K, Tammik C, Rosendahl K, Zetterberg E, Ringdén O. HLA expression and immunologic properties of differentiated and undifferentiated mesenchymal stem cells. *Exp Hematol*. 2003;31(10):890–896.
23. Chin KY. A review on the relationship between aspirin and bone health. *J Osteoporos*. 2017;2017:3710959.
24. Lee BS, Lee CC, Wang YP, Chen HJ, Lai CH, Hsieh WL, Chen YW. Controlled-release of tetracycline and lovastatin by poly(D,L-lactide-co-glycolide acid)-chitosan nanoparticles enhances periodontal regeneration in dogs. *Int J Nanomedicine*. 2016;11:285–297.
25. Lavie CJ, Howden CW, Scheiman J, Tursi J. Upper gastrointestinal toxicity associated with long-term aspirin therapy: consequences and prevention. *Curr Probl Cardiol*. 2017;42(5):146–164.
26. Magierowski M, Hubalewska-Mazgaj M, Magierowska K, Wojcik D, Sliwowski Z, Kwiecien S, Brzozowski T. Nitric oxide, afferent sensory nerves, and antioxidative enzymes in the mechanism of protection mediated by tricarbonyldichlororuthenium(II) dimer and sodium hydrosulfide against aspirin-induced gastric damage. *J Gastroenterol*. Epub 2017 Feb 25.
27. Elkhoul AM. The efficacy of host response modulation therapy (omega-3 plus low-dose aspirin) as an adjunctive treatment of chronic periodontitis (clinical and biochemical study). *J Periodontol Res*. 2011; 46(2):261–268.
28. Slots J, Ting M. Systemic antibiotics in the treatment of periodontal disease. *Periodontol 2000*. 2002;28:106–176.
29. Wei JS, Zeng R, Chen SY, Lin H, Wu SK, Zheng JC. Effects of aspirin on fracture healing in OPF rats. *Asian Pac J Trop Med*. 2014;7(10): 801–805.
30. Pountos I, Georgouli T, Calori GM, Giannoudis PV. Do nonsteroidal anti-inflammatory drugs affect bone healing? A critical analysis. *ScientificWorldJournal*. 2012;2012:606404.
31. Krayner JW, Leite RS, Kirkwood KL. Non-surgical chemotherapeutic treatment strategies for the management of periodontal diseases. *Dent Clin North Am*. 2010;54(1):13–33.
32. Shiloah J, Bland PS, Scarbecz M, Patters MR, Stein SH, Tipton DA. The effect of long-term aspirin intake on the outcome of non-surgical periodontal therapy in smokers: a double-blind, randomized pilot study. *J Periodontol Res*. 2014;49(1):102–109.
33. Muller M, Raabe O, Addicks K, Wenisch S, Arnhold S. Effects of non-steroidal anti-inflammatory drugs on proliferation, differentiation and migration in equine mesenchymal stem cells. *Cell Biol Int*. 2011; 35(3):235–248.
34. Joshi D, Garg T, Goyal AK, Rath G. Advanced drug delivery approaches against periodontitis. *Drug Deliv*. 2016;23(2):363–377.
35. Agnihotri SA, Mallikarjuna NN, Aminabhavi TM. Recent advances on chitosan-based micro- and nanoparticles in drug delivery. *J Control Release*. 2004;100(1):5–28.
36. Gopferich A. Mechanisms of polymer degradation and erosion. *Biomaterials*. 1996;17(2):103–114.
37. Saravanan S, Leena RS, Selvamurugan N. Chitosan based biocomposite scaffolds for bone tissue engineering. *Int J Biol Macromol*. 2016; 93(Pt B):1354–1365.
38. Kim BS, Kim JS, Lee J. Improvements of osteoblast adhesion, proliferation, and differentiation in vitro via fibrin network formation in collagen sponge scaffold. *J Biomed Mater Res A*. 2013;101(9):2661–2666.
39. Wang X, You C, Hu X, et al. The roles of knitted mesh-reinforced collagen-chitosan hybrid scaffold in the one-step repair of full-thickness skin defects in rats. *Acta Biomater*. 2013;9(8):7822–7832.
40. Wang Y, Van Manh N, Wang H, Zhong X, Zhang X, Li C. Synergistic intrafibrillar/extrafibrillar mineralization of collagen scaffolds based on a biomimetic strategy to promote the regeneration of bone defects. *Int J Nanomedicine*. 2016;11:2053–2067.
41. Qiu J, Li J, Wang G, et al. In vitro investigation on the biodegradability and biocompatibility of genipin cross-linked porcine acellular dermal matrix with intrinsic fluorescence. *ACS Appl Mater Interfaces*. 2013; 23;5(2):344–350.
42. Usha R, Sreeram KJ, Rajaram A. Stabilization of collagen with EDC/NHS in the presence of L-lysine: a comprehensive study. *Colloids Surf B Biointerfaces*. 2012;1;90:83–90.
43. Raftery RM, Woods B, Marques AL, et al. Multifunctional biomaterials from the sea: Assessing the effects of chitosan incorporation into collagen scaffolds on mechanical and biological functionality. *Acta Biomater*. 2016;43:160–169.
44. Cao Y, Xiong J, Mei S, Wang F, Zhao Z, Wang S, Liu Y. Aspirin promotes bone marrow mesenchymal stem cell-based calvarial bone regeneration in mini swine. *Stem Cell Res Ther*. 2015;6:210.
45. Shi S, Gronthos S, Chen S, Reddi A, Counter CM, Robey PG, Wang CY. Bone formation by human postnatal bone marrow stromal stem cells is enhanced by telomerase expression. *Nat Biotechnol*. 2002;20(6): 587–591.
46. Schmitz JP, Hollinger JO. The critical size defect as an experimental model for craniomandibulofacial nonunions. *Clin Orthop Relat Res*. 1986;205:299–308.
47. Liu Y, Wang L, Kikui T, et al. Mesenchymal stem cell-based tissue regeneration is governed by recipient T lymphocytes via IFN-gamma and TNF-alpha. *Nat Med*. 2011;17(12):1594–1601.
48. Jeon O, Song SJ, Kang SW, Putnam AJ, Kim BS. Enhancement of ectopic bone formation by bone morphogenetic protein-2 released from a heparin-conjugated poly(L-lactic-co-glycolic acid) scaffold. *Biomaterials*. 2007;28(17):2763–2771.



**International Journal of Nanomedicine****Dovepress****Publish your work in this journal**

The International Journal of Nanomedicine is an international, peer-reviewed journal focusing on the application of nanotechnology in diagnostics, therapeutics, and drug delivery systems throughout the biomedical field. This journal is indexed on PubMed Central, MedLine, CAS, SciSearch®, Current Contents®/Clinical Medicine,

Journal Citation Reports/Science Edition, EMBase, Scopus and the Elsevier Bibliographic databases. The manuscript management system is completely online and includes a very quick and fair peer-review system, which is all easy to use. Visit <http://www.dovepress.com/testimonials.php> to read real quotes from published authors.

Submit your manuscript here: <http://www.dovepress.com/international-journal-of-nanomedicine-journal>